ORIGINAL ARTICLE

Role of estrogen signaling in fibroblastic reticular cells for innate and adaptive immune responses in antigen-induced arthritis

Aidan Barrett[1], Karin Horkeby[2], Carmen Corciulo[3], Hans Carlsten[1], Marie K Lagerquist[2], Julia M Scheffler[1] & Ulrika Islander[1,4]

1 Department of Rheumatology and Inflammation Research, Institute of Medicine, Sahlgrenska Academy, University of Gothenburg, Gothenburg, Sweden
2 Department of Internal Medicine and Clinical Nutrition, Institute of Medicine, Sahlgrenska Osteoporosis Center, Centre for Bone and Arthritis Research, Sahlgrenska Academy, University of Gothenburg, Gothenburg, Sweden
3 Department of Pharmacology, Institute of Neuroscience and Physiology, Sahlgrenska Academy, University of Gothenburg, Gothenburg, Sweden
4 SciLifeLab, University of Gothenburg, Gothenburg, Sweden

Abstract

Women are more prone to develop rheumatoid arthritis, with peak incidence occurring around menopause. Estrogen has major effects on the immune system and is protective against arthritis. We have previously shown that treatment with estrogen inhibits inflammation and joint destruction in murine models of arthritis, although the mechanisms involved remain unclear. Fibroblastic reticular cells (FRCs) are specialized stromal cells that generate the three-dimensional structure of lymph nodes (LNs). FRCs are vital for coordinating immune responses from within LNs and are characterized by the expression of the chemokine CCL19, which attracts immune cells. The aim of this study was to determine whether the influence of estrogen on innate and adaptive immune cells in arthritis is mediated by estrogen signaling in FRCs. Conditional knockout mice lacking estrogen receptor α (ERα) in CCL19-expressing cells (Ccl19-CreER$\alpha^{fl/fl}$) were generated and tested. Ccl19-CreER$\alpha^{fl/fl}$ mice and littermate controls were ovariectomized, treated with vehicle or estradiol and subjected to the 28-day-long antigen-induced arthritis model to enable analyses of differentiated T- and B-cell populations and innate cells in LNs by flow cytometry. The results reveal that while the response to estradiol treatment in numbers of FRCs per LN is significantly reduced in mice lacking ERα in FRCs, estrogen does not inhibit joint inflammation or markedly affect immune responses in this arthritis model. Thus, this study validates the Ccl19-CreER$\alpha^{fl/fl}$ strain for studying estrogen signaling in FRCs within inflammatory diseases, although the chosen arthritis model is deemed unsuitable for addressing this question.

INTRODUCTION

The autoimmune disease rheumatoid arthritis (RA) afflicts up to 1% of the population.[1] The typical manifestation of RA includes massive infiltration by a variety of immune cells into the joints, which causes synovitis and destruction of cartilage and bone.[2] Women are more likely to develop the disease (female-to-male ratio 3:1) and the peak incidence of RA in women coincides with menopause, when the levels of endogenously produced estrogens rapidly drop.[3] Clinical studies evaluating the effects of hormone replacement therapy on disease severity in postmenopausal patients with RA are inconclusive, but reduced disease activity has been reported.[4–6] Hormone replacement therapy users were also shown to have a decreased risk of developing

seropositive RA.[7] Furthermore, a decrease in RA symptom severity has been reported during pregnancy, when estrogen is elevated.[8] Together, these studies suggest a protective role for estrogens in the development and progression of RA, but the immunological mechanisms involved remain unclear.

A protective effect of estrogen has been demonstrated in several murine arthritis models.[9,10] We showed previously that treatment of ovariectomized (OVX) mice with 17β-estradiol (E2) resulted in decreased disease development and symptom severity compared with vehicle (Veh) in the collagen antibody–induced arthritis model.[11] Similarly, in the collagen-induced arthritis model, treatment of OVX mice with E2 or an estrogen receptor α (ERα) agonist resulted in lower disease frequency and severity compared with controls.[12] The same outcome was also observed in the 14-day-long antigen-induced arthritis model (AIA-14d), where we could show that E2 treatment resulted in reduced joint destruction, decreased infiltration of neutrophils and macrophages to the synovium and lower $CD4^+$ T-cell proportions in the spleen.[13] In addition, E2 has been shown to reduce the production of proinflammatory cytokines including interleukin 1 beta (IL-1β), IL-6 and tumor necrosis factor alpha (TNFα).[14]

It is well established that estrogen can influence the development, activation and function of the immune system and can exert both pro- and anti-inflammatory effects dependent on the setting.[14,15] Estrogen inhibits both T and B lymphopoiesis,[16–18] but studies using T- or B-cell–specific ERα knockout mice revealed that the effects are not mediated by direct signaling in T or B cells.[19,20] Furthermore, E2 increases the production of antibodies from B cells in lymphoid organs.[21] We could show in the collagen-induced arthritis model that the E2-induced inhibition of joint inflammation was associated with retention of T helper 17 (Th17) cells in lymph nodes (LNs), and decreased number of Th17 cells in the joints.[22] These findings indicate that E2 influences the activation, differentiation and function of both T and B cells in LNs during arthritis, but the cell type involved in mediating these effects is still unknown.

The three-dimensional structure and different microenvironmental niches of LNs are generated by specialized stromal cells called fibroblastic reticular cells (FRCs). These cells are characterized by their expression of the chemokines CCL19 and CCL21 that attract CCR7-expressing immune cells to the LNs.[23] Intense research conducted over the past decade has revealed the importance of FRCs in coordinating immune functions, including T-cell migration in and out of the LNs[24–27]; facilitating interactions between dendritic cells (DCs), T cells and B cells; and maintaining the LN macrophage niche.[27–29] LN stromal cells have also been shown to support the maturation of conventional DCs (cDCs).[30] Medullary sinus macrophages (MSMs) and subcapsular sinus macrophages (SSMs) are capable of antigen presentation to other cell types within their respective LN niches.[31] While SSMs can present antigens to T cells as well as B cells, it has been shown that MSMs have a greater innate ability to process antigens.[32] By contrast, medullary cord macrophages (MCMs) are known producers of both IL-6 and a proliferation-inducing ligand (APRIL) and are important for the maintenance of surrounding lymphocyte populations.[31] However, it is not known how estrogen signaling in FRCs influences the ability of the cells to initiate, maintain and coordinate innate and adaptive immune responses during arthritis. Given our previous publications showing that estrogen ameliorates inflammation and joint destruction in experimental models of arthritis, the aim of this study was to determine the influence of estrogen signaling in FRCs for the regulation of innate and adaptive immune cells in arthritis. The 28-day long antigen-induced arthritis model (AIA-28d) was chosen to enable analyses of differentiated lymphocyte populations in LNs of mice with a C57BL/6 background. A comprehensive profiling of LN-resident macrophages and cDCs, as well as T- and B-cell populations was conducted to provide a thorough overview of the immune response within the LN microenvironment in the AIA-28d model. The results reveal that the response to E2 treatment in number of FRCs is significantly decreased in mice lacking ERα in FRCs, but E2 does not inhibit joint inflammation or markedly affect immune responses in the AIA-28d model.

RESULTS

Antigen-induced arthritis influences the levels of innate and adaptive immune cells in lymph nodes

To define immunological responses induced by the AIA model, female C57BL/6J mice were immunized and challenged with antigens in the knee joint according to the timeline shown in Figure 1a. Daily measurement of knee swelling showed that the knee joints from AIA-challenged mice (AIA) were significantly more swollen compared with those of healthy controls (HCs) when comparing areas under the curve (days 21–28) (Figure 1b). AIA mice also had an increased number of cells per skin-draining LN compared with HCs (Figure 1c). Analysis of LN-resident macrophage populations showed that AIA mice had increased numbers of MCMs, SSMs as well as MSMs per LN compared with HCs (Figure 1d–f). The gating strategy for LN macrophages is shown in Supplementary figure 1.
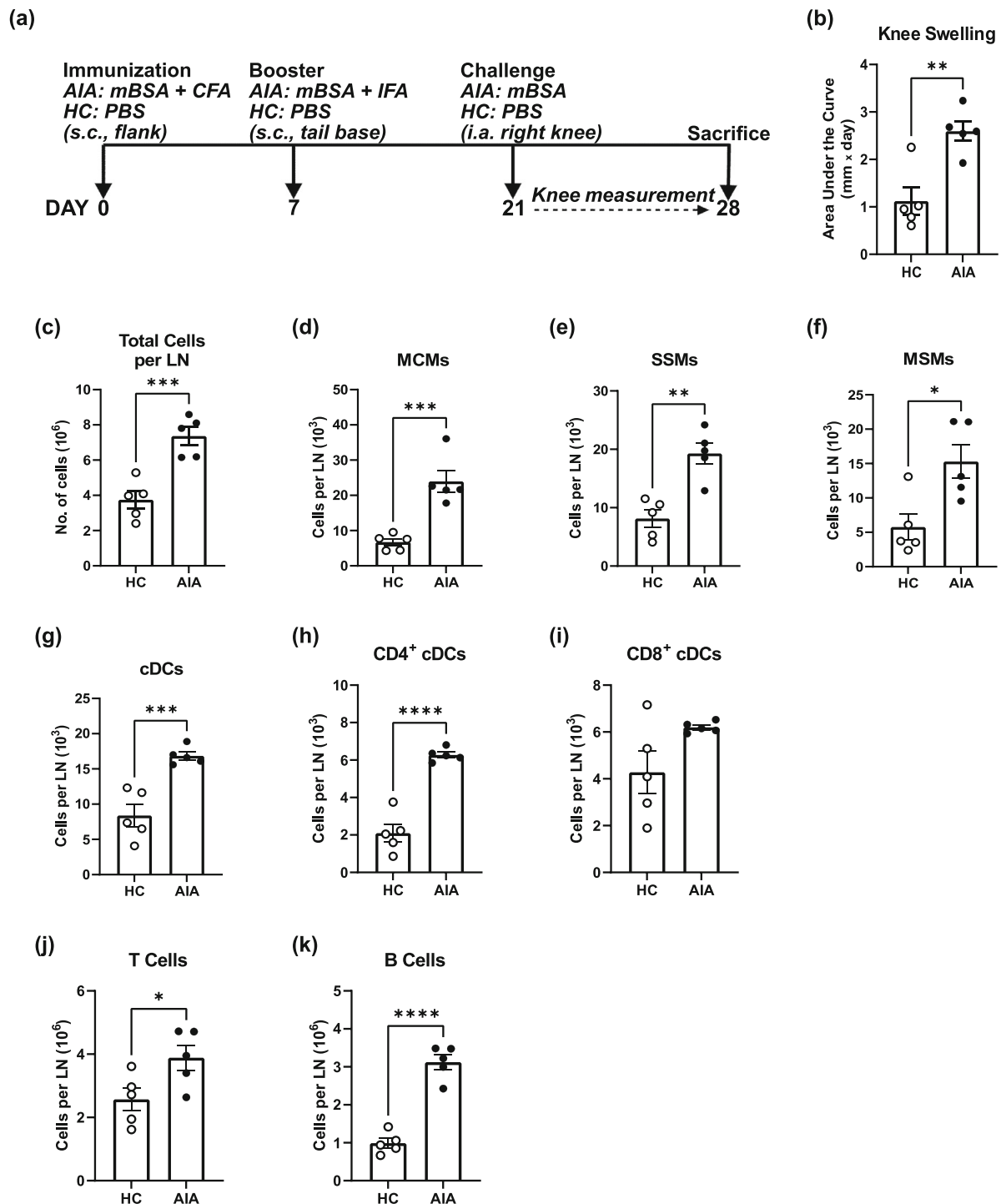
Figure 1. Antigen-induced arthritis (AIA) induces changes in both innate and adaptive immune cell populations in lymph nodes (LNs). Ten-week-old female wild-type C57BL/6J mice were immunized and boosted systemically, then challenged locally in the right knee joint with methylated bovine serum albumin (mBSA; AIA). Healthy controls (HCs) received PBS in equal volumes at all stages. **(a)** Experiment outline. **(b)** Area under the curve for knee swelling (day 21–28) of HCs and mice subjected to AIA. **(c)** Total number of cells per skin-draining LN. Flow cytometry was performed on LN cells to determine the total cell number per LN of **(d)** medullary cord macrophages (MCMs), **(e)** medullary sinus macrophages (MSMs), **(f)** subcapsular sinus macrophages (SSMs), **(g)** conventional dendritic cells (cDCs), **(h)** CD4+ cDCs, **(i)** CD8+ cDCs, **(j)** T cells and **(k)** B cells. Data are presented as mean ± standard error of the mean, $n = 5$ mice per group, data from one experiment. Unpaired two-tailed Student's *t*-test, *$P < 0.05$; **$P < 0.01$; ***$P < 0.001$; ****$P < 0.0001$. CFA, complete Freund's adjuvant; IFA, incomplete Freund's adjuvant; i.a., intra-articular; s.c., subcutaneous

The total number of cDCs per LN increased significantly after AIA compared with HCs (Figure 1g). Of these, the increase in the number of CD4$^+$ cDCs was prominent, but there was no difference in the number of CD8$^+$ cDCs compared with HCs (Figure 1h, i). The gating strategy for LN cDCs is shown in Supplementary figure 2. In addition, AIA mice had increased numbers of both T and B cells in LNs compared with HCs (Figure 1j, k).

Deletion of *ER*α in FRCs does not affect FRC number, activation status or LN architecture at steady state

The FRC phenotype and LN architecture of Ccl19-Cre *ER*α$^{fl/fl}$ mice and *ER*α$^{fl/fl}$ littermate controls were quantified at steady state. Under healthy conditions, the number of FRCs per skin-draining LNs did not differ between the genotypes (Figure 2a). Likewise, expression of the activation markers major histocompatibility complex class I (MHCI) and II (MHCII), CD40, CD80, CD86, programmed death-ligand 1 (PD-L1) or programmed death-ligand 2 (PD-L2) on FRCs were unaltered between genotypes (Figure 2b–h). Messenger RNA (mRNA) expression of the ERα gene *Esr1* was determined in cultured FRCs from Ccl19-Cre *ER*α$^{fl/fl}$ mice and controls. Unstimulated FRCs isolated from Ccl19-Cre *ER*α$^{fl/fl}$ mice show a trend toward downregulation of *Esr1* mRNA compared with *ER*α$^{fl/fl}$, and the difference was significant in cells that were stimulated with E2 (Figure 2i, j). Immunohistological staining and confocal imaging of whole LNs show that the structural integrity of the LNs is maintained when ERα is conditionally deleted in FRCs (Figure 2k).

E2 affects the number of FRCs in an ERα-dependent manner during AIA-28d

A previous study from our laboratory showed that treatment with estrogen inhibits synovitis and joint destruction in mice subjected to the AIA-14d model.[13] To investigate whether the effect of estrogen on differentiated immune cells in arthritis is mediated via FRCs, Ccl19-Cre *ER*α$^{fl/fl}$ and *ER*α$^{fl/fl}$ mice were OVX, treated with Veh or E2 and subjected to the AIA-28d model. The experimental outline is summarized in Figure 3a. Two-way ANOVA followed by Tukey's *post hoc* multiple comparison test was used to compare genotypes (*ER*α$^{fl/fl}$ and Ccl19-Cre *ER*α$^{fl/fl}$) and treatment groups (Veh and E2). *P* values for differences as a result of E2 treatment (T), genotype (G) or difference in treatment response between genotypes (Int) from the two-way ANOVA are shown next to each graph. The uterus weight was substantially increased after E2 treatment in both genotypes (Figure 3b). As expected, the antigen-injected

knee (AIA knee) had increased in size compared with the PBS-injected control knee (PBS knee) for both genotypes and treatment groups (Supplementary figure 3a). However, knee swelling, analyzed as an area under the curve (AUC) (days 21–28), revealed no significant differences between genotypes or treatment groups (Figure 3c; Supplementary figure 3a). Furthermore, histological examination of synovial thickness and cellular infiltration of the AIA knee revealed no significant differences in the histopathological score between E2- and Veh-treated mice of either genotype (Supplementary figure 3b, c). Both E2 treatment and genotype significantly influenced the total number of cells per LN (Figure 3d). The effects of estrogen on the numbers of the LN stromal cell populations (FRCs, blood endothelial cells (BEC) and lymphatic endothelial cells (LEC) were determined by flow cytometry. The gating strategy for FRCs, BEC and LEC is shown in Supplementary figure 4. The total number of FRCs per LN was significantly decreased after E2 treatment in Ccl19-Cre *ER*α$^{fl/fl}$ mice compared with controls, and the difference in treatment response between genotypes was confirmed by a significant interaction (Int) *P*-value according to the two-way ANOVA (Figure 3e). A significant genotype difference was observed in the total numbers of BEC per LN (Figure 3f), while no differences in the numbers of LECs between groups were found (Figure 3g). Mean fluorescent intensity (MFI) (normalized to *ER*α$^{fl/fl}$/Veh) of the activation markers MHCII, CD40, CD86 or PD-L1 on FRCs was not altered in response to treatment or genotype (Figure 3h–k).

The response to E2 treatment in numbers of LN macrophages and cDCs does not differ between genotypes during AIA-28d

Flow cytometry analysis of LN macrophage and DC populations was performed to characterize the influence of estrogen signaling in FRCs on innate immune cells in LNs. Overall differences between genotypes were observed for numbers of MCM and MSM (Figure 4a, b), and a significant treatment effect was shown for numbers of SSM per LN (Figure 4c). E2 treatment resulted in significantly decreased numbers of cDCs per LN in both genotypes (Figure 4d). No differences were observed in the expression of the DC activation markers MHCII or CD40 on cDCs in response to treatment or between genotypes (Figure 4e, f). The expression of CD86 on cDCs was significantly affected by both E2 treatment and the genotype of the mice (Figure 4g). Numbers of CD4$^+$ cDCs in LNs were also decreased by E2 treatment in both genotypes (Supplementary figure 5a). Expression of MHCII on CD4$^+$ cDCs normalized to *ER*α$^{fl/fl}$/Veh was
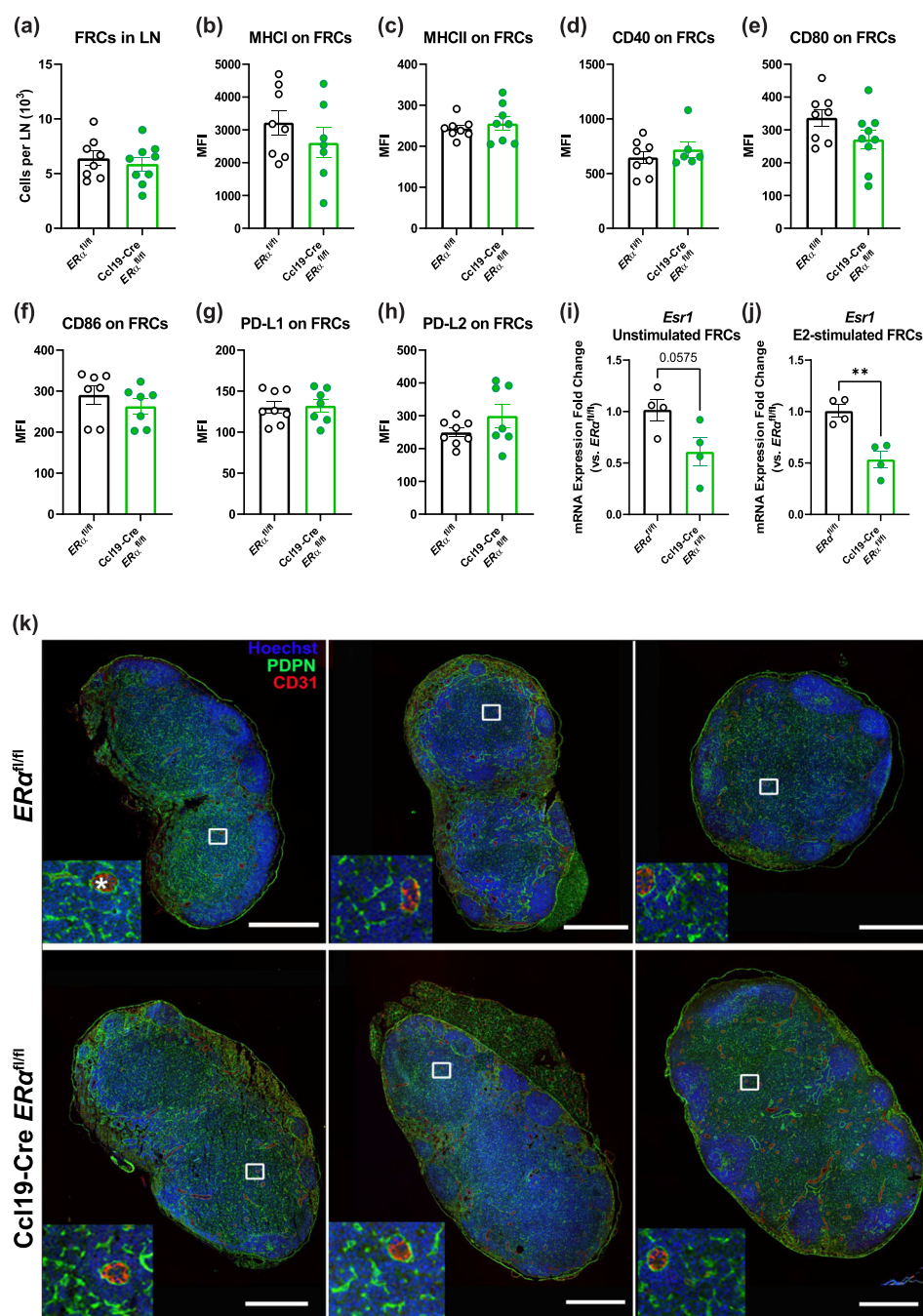
Figure 2. Total numbers of fibroblastic reticular cells (FRCs), expression of activation markers and lymph node (LN) architecture are unaltered in healthy Ccl19-Cre $ER\alpha^{fl/fl}$ mice. Skin-draining LNs were harvested from 11- to 15-week-old female Ccl19-Cre $ER\alpha^{fl/fl}$ and littermate controls ($ER\alpha^{fl/fl}$), digested and analyzed by flow cytometry. Total number of cells per LN of **(a)** FRCs. Mean fluorescent intensity on FRCs of **(b)** major histocompatibility complex class I (MHCI), **(c)** MHCII, **(d)** CD40, **(e)** CD80, **(f)** CD86, **(g)** programmed death-ligand 1 (PD-L1) and **(h)** programmed death-ligand 2 (PD-L2). Data are presented as mean ± standard error of the mean, $n = 6-9$ mice per group, data from one experiment, unpaired two-tailed Student's t-test. For quantification of expression of the estrogen receptor alpha gene (Esr1), FRCs from skin-draining LNs of 12–16-week-old male Ccl19-Cre $ER\alpha^{fl/fl}$ and littermate controls ($ER\alpha^{fl/fl}$) were cultured for 6–8 days, and then for a further 24 h either unstimulated or stimulated with 1×10^{-8} M estradiol (E2). RNA was extracted from the cells and real-time PCR was performed. Fold change in Esr1 expression compared with $ER\alpha^{fl/fl}$ from **(i)** unstimulated FRCs and **(j)** E2-stimulated FRCs. Data are presented as mean ± standard error of the mean, $n = 4$ mice per group, data from one experiment. Student's t-test, **$P < 0.01$. **(k)** Confocal imaging of whole LNs stained with Hoechst DNA stain (blue), podoplanin (PDPN; green) and CD31 (red). The white star denotes a high endothelial venule. The scale bar is 500 µm. ERα, estrogen receptor α; MFI, mean fluorescent intensity.
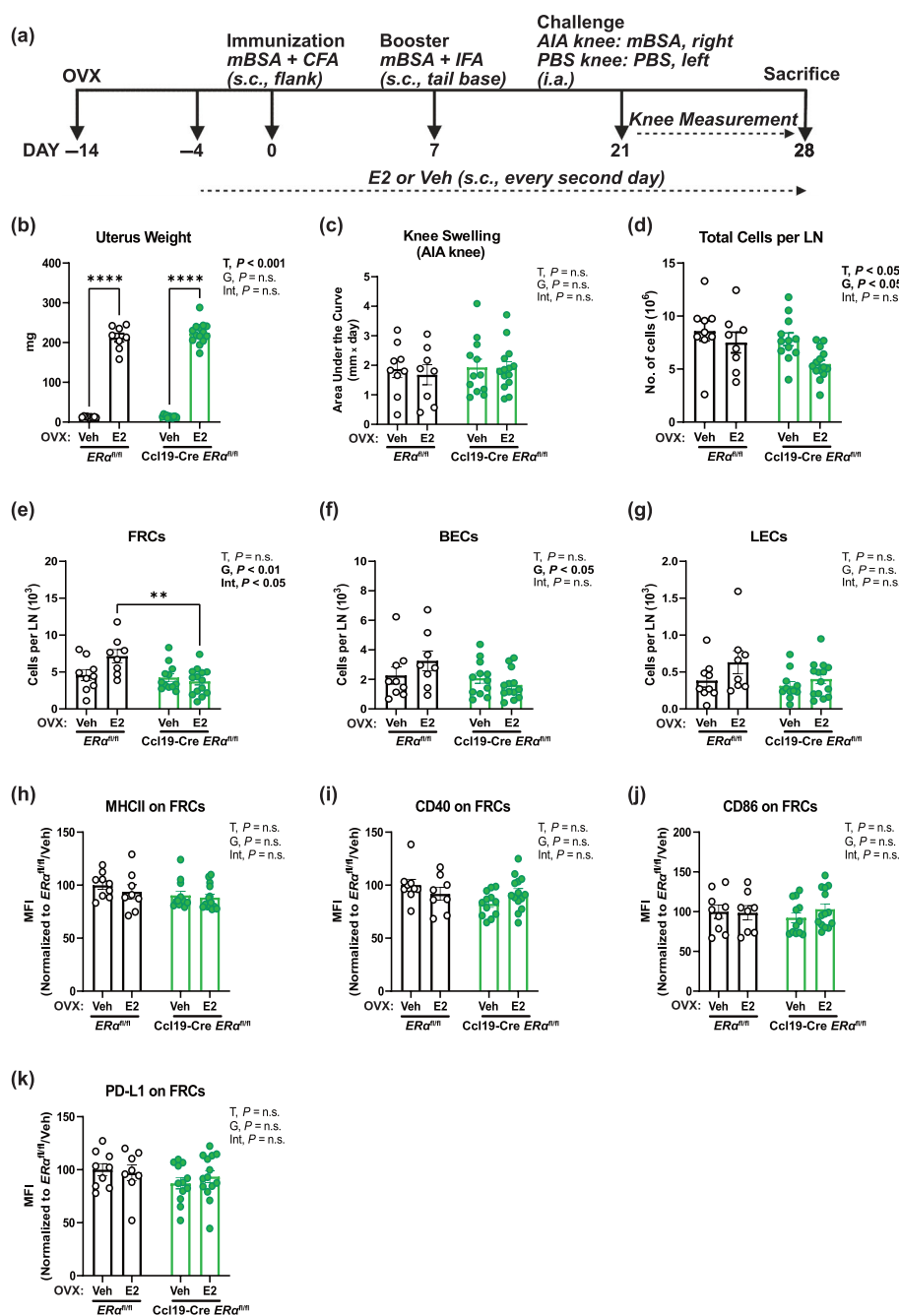
Figure 3. Estradiol (E2) affects the number of fibroblastic reticular cells (FRCs) in an estrogen receptor α (ERα)-dependent manner during antigen-induced arthritis (AIA). Eight-week-old female Ccl19-Cre *ERα*^fl/fl and littermate controls (*ERα*^fl/fl) were ovariectomized (OVX) and treated with either E2 or vehicle (Veh). Two weeks after OVX, mice were subjected to the AIA-28d immunization protocol and challenged with antigen in the right knee (AIA knee) and PBS in the left (PBS knee). The experiment outline is shown in **a**. **(b)** Uteri were weighed to confirm successful OVX and E2 treatment. **(c)** Area under the curve (AUC) for knee swelling (days 21–28) of the AIA knee. **(d)** Total number of cells per skin-draining lymph node (LN). Total numbers of cells per LN of **(e)** FRCs, **(f)** blood endothelial cells (BECs) and **(g)** lymphatic endothelial cells (LECs). Mean fluorescent intensity (MFI) of **(h)** major histocompatibility complex class II (MHCII), **(i)** CD40 **(j)** CD86 and **(k)** programmed death-ligand 1 (PD-L1) on FRCs, normalized to the mean value of the *ERα*^fl/fl/Veh-treated group (shown as %). Data are presented as mean ± standard error of the mean, $n = 8$–14 mice per group, data pooled from two experiments. Two-way ANOVA followed by Tukey's multiple comparison test, **** $P < 0.0001$. G, genotype; Int, interaction term; mBSA, methylated bovine serum albumin; n.s., nonsignificant; s.c., subcutaneous; T, treatment.
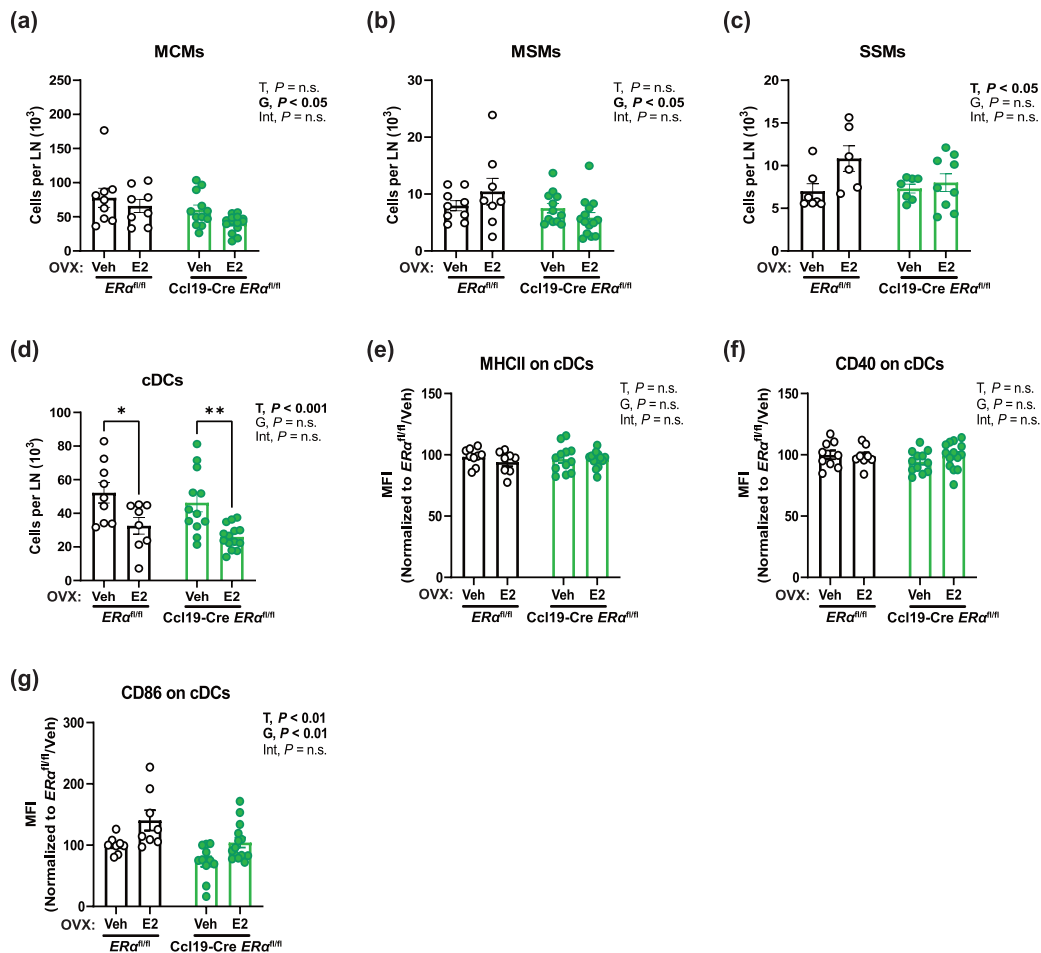
Figure 4. The response to estradiol (E2) treatment in numbers of lymph node macrophages and conventional dendritic cells (cDCs) does not differ between genotypes during antigen-induced arthritis (AIA). Eight-week-old female Ccl19-Cre *ERα*^fl/fl and littermate controls (*ERα*^fl/fl) were ovariectomized (OVX) and treated with either E2 or vehicle (Veh). Two weeks after OVX, mice were subjected to the AIA-28d immunization protocol and challenged with antigen in the right knee (AIA knee) and PBS in the left (PBS knee). Number of cells per lymph node (LN) of **(a)** medullary cord macrophages (MCMs), **(b)** medullary sinus macrophages (MSMs) and **(c)** subcapsular sinus macrophages (SSMs). Number of cells per LN of **(d)** cDCs. Mean fluorescent intensity (MFI) of **(e)** major histocompatibility complex class II (MHCII), **(f)** CD40 and **(g)** CD86 on cDCs, normalized to the mean value of the *ERα*^fl/fl/Veh-treated group (shown as %). Data are presented as mean ± standard error of the mean, $n = 8–14$ mice per group, data pooled from two experiments. Two-way ANOVA followed by Tukey's multiple comparison test, *$P < 0.05$; **$P < 0.01$. ERα, estrogen receptor α; G, genotype; Int, interaction term; n.s., nonsignificant; T, treatment.

not affected by treatment or genotype (Supplementary figure 5b), but there was an overall treatment effect in the expression of CD40 and CD86 on CD4^+ cDCs (Supplementary figure 5c, d). Total numbers of CD8^+ cDCs per LN were also decreased by treatment with E2 in both genotypes (Supplementary figure 5e). Normalized expression of MHCII and CD40 on CD8^+ cDCs was not affected by E2 treatment or genotype (Supplementary figure 5f, g). However, the expression of CD86 on CD8^+ cDCs was significantly influenced by both E2 treatment and genotype of the mice (Supplementary figure 5h).

The response to E2 treatment in numbers of T cells does not differ between genotypes during AIA-28d

T-cell populations in LNs of mice with AIA-28 were analyzed by flow cytometry. The gating strategy for T-cell subpopulations is shown in Supplementary figure 6. Treatment with E2 decreased the numbers of total T cells and CD4^+ T cells in the LNs of both *ERα*^fl/fl and Ccl19-Cre *ERα*^fl/fl mice (Figure 5a, b). An overall treatment effect in the number of CD8^+ T cells per LN (Figure 5c) was found, while the numbers of Th1 cells
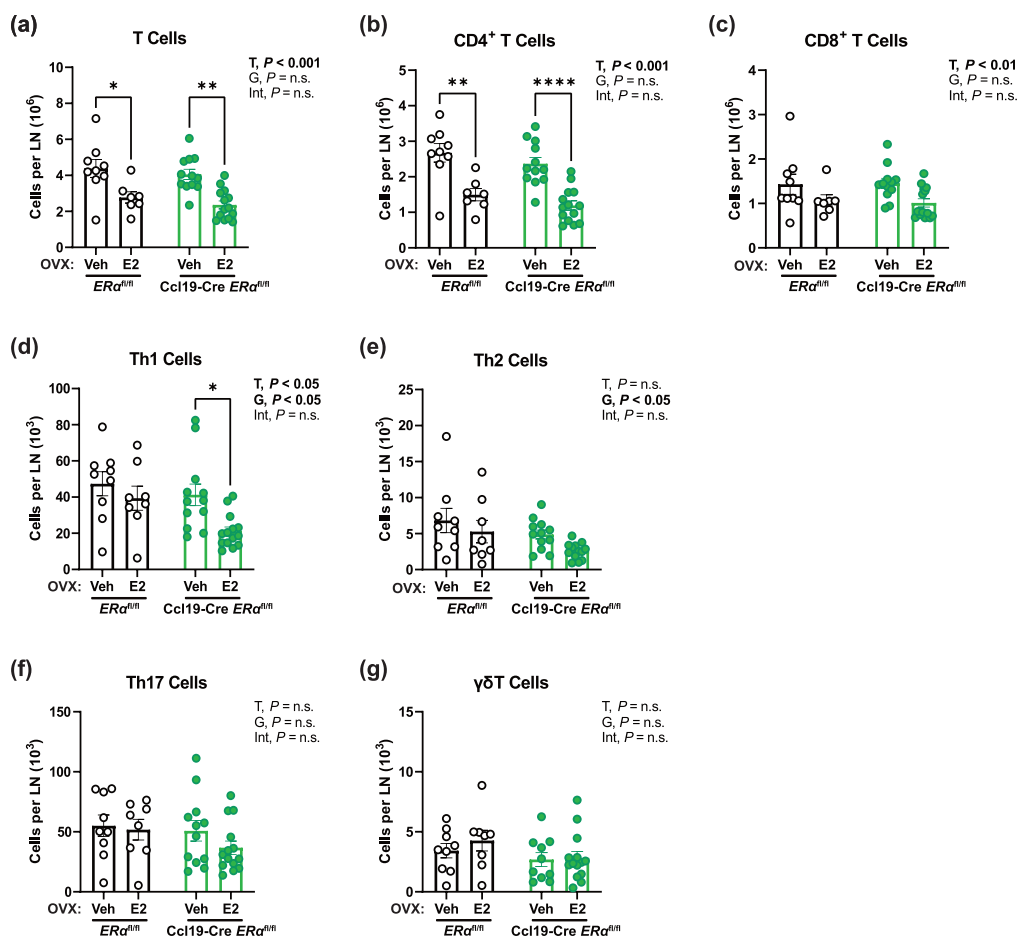
Figure 5. The response to estradiol (E2) treatment in numbers of T cells in lymph nodes during antigen-induced arthritis (AIA) does not differ between genotypes. Eight-week-old female Ccl19-Cre $ER\alpha^{fl/fl}$ and littermate controls ($ER\alpha^{fl/fl}$) were ovariectomized (OVX) and treated with either E2 or vehicle (Veh). Two weeks after OVX, mice were subjected to the AIA-28d model and skin-draining lymph nodes (LNs) were collected at the termination of the experiment. T-cell populations were examined by flow cytometry. Number of cells per LN of **(a)** T cells, **(b)** CD4+ T cells and **(c)** CD8+ T cells. Number of cell numbers per LN of **(d)** T helper 1 (Th1) cells, **(e)** Th2 cells, **(f)** Th17 cells and **(g)** γδT cells. Data are presented as mean ± standard error of the mean, $n = 8$–14 mice per group, data pooled from two experiments. Two-way ANOVA followed by Tukey's multiple comparison test, *$P < 0.05$; **$P < 0.01$; ****$P < 0.0001$. ERα, estrogen receptor α; G, genotype; Int, interaction term; n.s., nonsignificant; T, treatment.

were significantly influenced by both E2 treatment and genotype (Figure 5d). Th2 cells were significantly affected by genotype (Figure 5e), while the numbers of Th17 and γδT cells per LN were not influenced by either treatment or genotype (Figure 5f, g).

The response to E2 treatment in numbers of B cells or plasma cells and production of antibodies does not differ between genotypes during AIA-28d

Quantification of B-cell populations in the LNs of mice with AIA was also performed by flow cytometry. The gating strategy for B-cell subpopulations is shown in Supplementary figure 7. The total number of B cells per LN was not affected by either E2 treatment or genotype (Figure 6a), while the numbers of plasma cells, plasmablasts, early plasma cells and mature resting plasma cells per LN were significantly affected by treatment but not by genotype (Figure 6b–e). The production of immunoglobulin (Ig)M and IgG from B cells was influenced by treatment with E2 but not by genotype in the AIA-28d model (Figure 6f, g). An analysis of inflammation-associated cytokines in serum at the termination of the experiment (day 28) revealed that
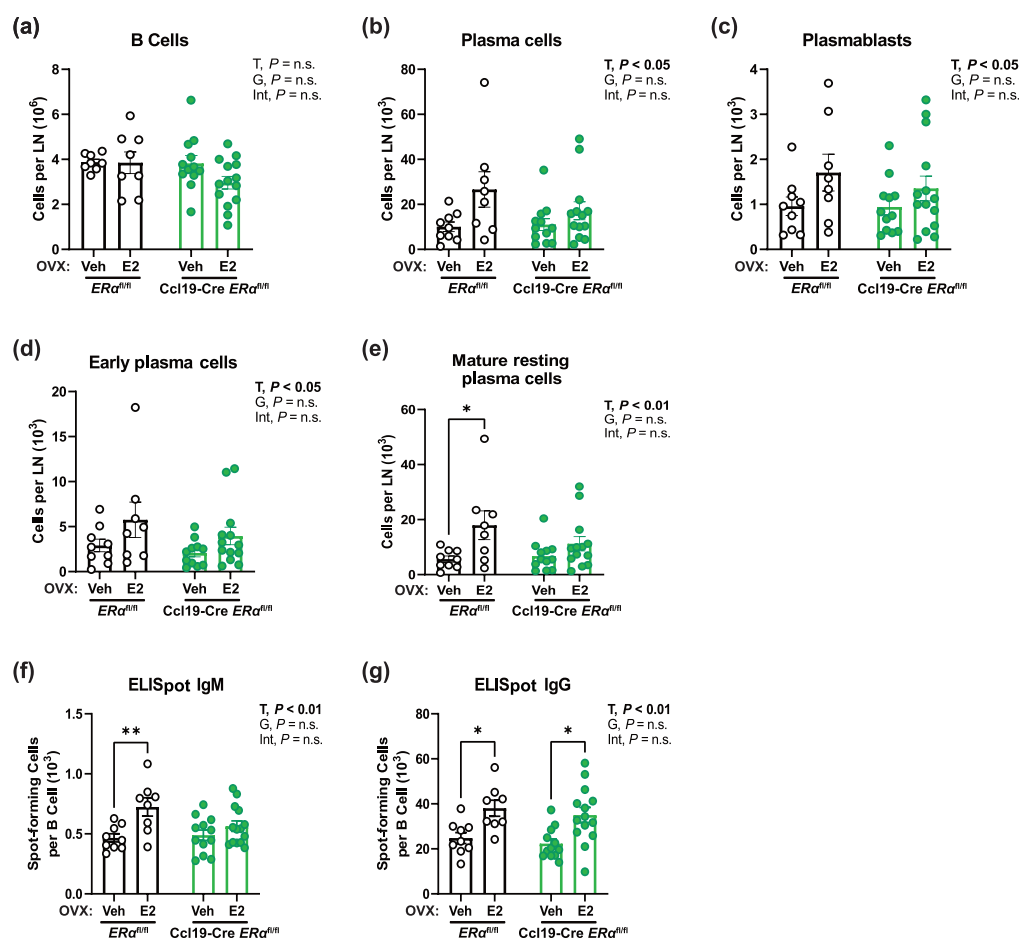
Figure 6. The response to estradiol (E2) treatment in numbers of plasma cells and immunoglobulin (Ig)-producing B cells in lymph nodes does not differ between genotypes. Eight-week-old female Ccl19-Cre ERα$^{fl/fl}$ and littermate controls (ERα$^{fl/fl}$) were ovariectomized (OVX) and treated with either E2 or vehicle (Veh). Two weeks after OVX, mice were subjected to the 28-day-long antigen-induced arthritis model (AIA-28d) model and skin-draining lymph nodes (LNs) were collected at the termination of the experiment. B-cell populations in LNs were analyzed with flow cytometry. Total numbers of cells per LN of **(a)** B cells, **(b)** plasma cells, **(c)** plasmablasts, **(d)** early plasma cells and **(e)** mature resting plasma cells. Enzyme-linked immunospot (ELISpot) assay analysis of **(f)** number of IgM-producing cells per 10^3 B cells in LNs and **(g)** number of IgG-producing cells per 10^3 B cells in LNs. Data are presented as mean ± standard error of the mean, $n = 7$–14 mice per group, data pooled from two experiments. Two-way ANOVA followed by Tukey's multiple comparison test, *$P < 0.05$; **$P < 0.01$. ERα, estrogen receptor α; G, genotype; Int, interaction term; n.s., nonsignificant; T, treatment.

the levels of IL-27 were affected by genotype (Supplementary figure 8j), but no differences were detected between the groups for any of the other cytokines (Supplementary figure 8a–i, k–n).

DISCUSSION

The anti-inflammatory effect of estrogen has previously been demonstrated in patients with RA and in animal models of arthritis.[4–10] However, the mechanism underpinning this phenomenon is not yet fully

understood. The aim of this study was to determine how estrogen signaling in LN FRCs affects innate and adaptive immune cells in arthritis using the AIA-28d model. Conditional knockout mice lacking ERα in CCL19-expressing cells (Ccl19-CreERα$^{fl/fl}$) were generated and validated. The results suggest that deletion of ERα in FRCs in healthy mice does not affect FRC number, activation status or LN architecture, while the response to E2 treatment in numbers of FRCs during AIA-28d is significantly decreased in mice that lack ERα in FRCs. Nevertheless, since E2 treatment failed to suppress joint

inflammation or induce expected effects on immune responses compared with Veh in the *ERα*$^{fl/fl}$ control mice, the AIA-28d model is deemed inadequate for addressing the primary research question.

To define changes in the LN immune cell composition induced by the AIA-28d model, female wild-type mice subjected to AIA were compared with HCs. As expected, knee swelling and LN cellularity increased upon the AIA challenge, confirming the success of the model in inducing joint inflammation in response to the antigen. In LNs, the numbers of MCMs, MSMs and SSMs increased after the AIA challenge. Further, increased numbers of cDCs, particularly CD4$^+$ cDCs, were observed. Numbers of T cells and B cells per LN both increased, further underlining the success of the model in inducing a multifaceted immune response and suggesting a change in the LN microenvironment in response to the antigen. The increased numbers of MSMs and MCMs in LNs of mice with AIA could result from the augmented need to present antigens within the LNs to propagate and maintain the immune response, but further studies are necessary to define the importance of these macrophage populations during arthritis. To our knowledge, this is the first study to quantify changes in LN macrophage populations in the AIA-28d model.

We have previously shown that E2 treatment inhibits synovitis and joint destruction in mice subjected to the AIA-14d model.[13] In this study, the AIA-28d model was used to enable the analysis of differentiated immune cell populations in LNs. However, to our surprise, E2 treatment of control mice did not result in reduced knee swelling or histopathological severity score compared with Veh. We speculate that the increased time span before antigen challenge in the knee joint in the AIA-28d model could have resulted in a weaker overall inflammation at the time of challenge, which obstructed the elucidation of larger histopathological differences. Another difference between the studies involves the administration of E2. In our previous study, E2 was administered in the form of a slow-release pellet, as opposed to a subcutaneous injection in this study. While the calculated average E2 dose per day is similar in both studies (0.83 μg/mouse/day in the previous study and 0.75 μg/mouse/day in this study), the kinetic profile of E2 release from the pellet may initially be high but decrease over time compared with the more stable regimen of subcutaneous injections every second day. Together, these factors could contribute to the difference in E2-related effects on joint pathology between the studies.

The importance of the FRC network in LNs for coordinating and aiding immune responses is well documented.[24–27,33–35] However, the effect of estrogen signaling via FRCs on immune responses in arthritis is unknown. Development of the Ccl19-Cre *ERα*$^{fl/fl}$ conditional knockout model allows us to establish the immunological effects of estrogen signaling via FRCs for immune responses in models of arthritis. Phenotyping of FRC number and activation status showed that lack of ERα does not affect FRC homeostasis or the architecture of the LNs at steady state. In the AIA-28d model, the number of FRCs differed significantly between genotypes in response to treatment, suggesting that estrogen propagates the proliferation of FRCs via ERα in inflammatory conditions. Thus, estrogen signaling via FRCs may be a factor in regulating the effects of estrogen on immune responses.

It was recently demonstrated that LN stromal cells support the maturation of precursor DCs into cDCs.[30] Further, it has been shown *in vitro* that E2-treated cDCs from lupus-prone B6.NZM Sle1/Sle2/Sle3 mice display increased immunometabolism, and that E2 is important in modulating their cytokine signature.[36] Although we could not elucidate any difference in response to E2 treatment between genotypes on cDCs in the AIA-28d model, it would be worth investigating whether the estrogenic effects on FRCs and cDCs are correlated in models of experimental lupus.

Our previous studies showed that the E2-induced inhibition of joint inflammation was associated with increased numbers of IL-17–producing T cells in LNs during collagen-induced arthritis.[22,37] Those results could not be repeated using the AIA-28d model, although a significant influence of E2 treatment on the numbers of different T-cell populations was found. Given the known importance of FRCs in coordinating T-cell responses in LNs, it would be worthwhile to study the link between estrogen, FRCs and T cells in another inflammatory setting.

The influence of estrogen on B-cell maturation and function is well known. E2 suppresses B-lymphocyte precursors in the bone marrow, but augments Ig production from mature B cells.[38] In addition, E2 has been shown to increase the number of plasma cells[39] as well as the production of both IgM and IgG in healthy mice.[39] In this study, the numbers of mature resting plasma cells, and IgM- and IgG-producing B cells in LNs, were significantly increased by E2 treatment in *ERα*$^{fl/fl}$ control mice, but two-way ANOVA revealed that the response to E2 treatment did not differ between genotypes. It has been suggested that a subset of FRCs located within the medullary region of the LNs, medullary FRCs, plays a role in maintaining plasma cell survival and function by local production of B-cell activating factor (BAFF), IL-6 and CXCL12.[40] As medullary FRCs also express Ccl19,[23] it is possible that

this specific FRC subpopulation can contribute to mediating the effects of E2 on plasma cells in LNs, although no such effect was shown using the AIA-28d model. BAFF can affect the survival of peripheral B cells,[41] and it has previously been demonstrated that treatment with E2 increases serum levels of BAFF in healthy mice.[21] We could not detect an increase in serum BAFF in this study, which could be due to the sampling timepoint, 7 days after the antigen challenge. It is possible that BAFF levels in serum spiked at an earlier timepoint, and it would be of interest to investigate whether BAFF levels correlate with the observed changes in B-cell populations at earlier timepoints using another arthritis model.

Overall, this study outlines an innovative method of studying a potential mechanism governing how estrogen regulates immune responses in a model of arthritis. As previously highlighted, E2 can ameliorate joint destruction in the AIA-14d model, but it was shown that this effect is not dependent on ERα signaling in chondrocytes.[13] In addition, a T-cell specific ERα knockout model showed that estrogen signaling in T cells was not a requirement for mediating the protective effects of estrogen on bone.[19] The effects of estrogen on different innate and adaptive immune cells have been demonstrated in different experimental models and settings, although the exact mechanisms are still unclear and context-dependent.[42,43] In this study, we tested the hypothesis that estrogen influences the immune response via LN FRCs in the AIA-28d model. The chosen arthritis model was deemed unsuitable for addressing this question because of the inability to induce well-described estrogen-mediated effects on immune cells and cytokine production. However, the transgenic mouse model provides an interesting and novel way of studying mechanisms of estrogenic regulation of the immune system in other disease settings.

METHODS

Animals

All mice were kept in cages (2–10 per cage) in pathogen-free conditions at 22°C, 12-h light/dark cycle and with *ad libitum* access to soy-free chow (Teklad diet 2016; Envigo, Indianapolis, IN, USA) and tap water. All experimental procedures were conducted with the approval of the regional ethical review board in Gothenburg (Dnr 4518/22) and in accordance with the European Union Directive 2010/63.

To compare HCs against mice subjected to the AIA-28d model, 10-week-old female C57BL/6J mice (Charles River, Göttingen, Germany) were used. For all following experiments, Ccl19-Cre mice (provided by Professor Burkhard Ludewig, Kantonsspital St. Gallen, St. Gallen, Switzerland)[44] crossed with *ERα*fl/fl mice (provided by Professor Jan-Åke Gustafsson,

University of Houston, TX, USA)[45] to generate Ccl19-Cre *ERα*fl/fl mice and *ERα*fl/fl littermate controls were used.

28-Day-long antigen-induced arthritis

Ten-week-old mice were immunized with 2 mg mL^{-1} of methylated bovine serum albumin (mBSA; Sigma Aldrich, Stockholm, Sweden) dissolved in phosphate-buffered saline (PBS; Gibco, Paisley, UK) and mixed with an equal volume of complete Freund's adjuvant (Chondrex, Woodinville, WA, USA) to create an emulsion. A volume of 100 μL of the emulsion was injected subcutaneously into each flank (200 μL total, 0.2 mg mBSA/mouse). HCs received injections with PBS.

Seven days after the first immunization, a booster immunization was administered. Here, 2 mg mL^{-1} mBSA was mixed with an equal volume of incomplete Freund's adjuvant (Chondrex) to create an emulsion. Fifty microliters of the emulsion was injected subcutaneously on either side of the base of the tail (100 μL total, 0.1 mg mBSA/mouse). HCs received injections with PBS.

Two weeks after the booster immunization, mice received an intra-articular injection of 30 μg mBSA dissolved in 20 μL of PBS into the right knee joint, and 20 μL of PBS into the left knee joint as a control. HCs received PBS in both knees.

The width of each knee joint was measured and recorded before injection using a caliper. Measurement of knee joint width was repeated every day for the following 7 days.

Ovariectomy and hormone treatment

Two weeks before the start of AIA immunization and challenge, female Ccl19-Cre *ERα*fl/fl and *ERα*fl/fl mice were anesthetized with isoflurane (Baxter Medical AB, Kista, Sweden) and ovariectomized as previously described.[22] In brief, a midline incision was made in the skin along the back followed by small incisions in the peritoneum to locate and remove the ovaries on either flank. The peritoneal incisions were sutured with absorbable suture thread (Agnthos, Lidingö, Sweden), and the skin incision was clamped and closed with metal reflex clips (Agnthos). All mice were given 100 μg/mouse of meloxicam (Metacam; Boehringer Ingelheim, Copenhagen, Denmark) subcutaneously as a preoperative analgesic.

Ten days after the surgery, mice were injected subcutaneously with either 17β-estradiol-3-benzoate (1.5 μg/mouse/injection; Sigma Aldrich) dissolved in miglyol (Miglyol812; Omya Peralta GmbH, Hamburg, Germany) or only miglyol (Veh). Repeat subcutaneous injections were administered every 2 days until the termination of the experiments.

Experiment termination and tissue collection

Seven days after the knee injection, mice were anesthetized with a mixture of dexmedetomidine (Dexdomitor vet; Orion Pharma, Sollentuna, Sweden) and ketamine (Ketador vet; Salfarm Scandinavia, Helsingborg, Sweden). Blood was collected in 1.1mL CAT-gel serum collection tubes (Sarstedt, Nümbrecht, Germany) by severance of the axillary artery,

followed by cervical dislocation. The serum was isolated and stored at –80°C until further analysis. The uterus was removed, perforated to remove excess liquid and weighed. Eight skin-draining LNs (the inguinal, axillary, brachial and one superficial cervical LN from each side) were removed and stored in cold PBS until further analysis. The right and left leg (femur and tibia) were excised, the foot and fur removed and the remaining joint placed in 4% paraformaldehyde.

Histological examination

After fixation in 4% paraformaldehyde for 2 days, the joints were washed with PBS and placed in 10% ethylenediaminetetraacetic acid (EDTA; prepared in-house) at pH 7.5. The EDTA solution was changed two times a week until the bones were fully decalcified, embedded in paraffin and sectioned at a thickness of 5 μm. Sections were stained with hematoxylin/eosin (Sigma Aldrich) and pictures were taken with a ZEISS Axioscan 7 microscope (Zeiss, Oberkochen, Germany). Synovial thickness and joint inflammation were separately scored from 0 to 3 (0 = unaffected, 1 = mild, 2 = moderate and 3 = severe) by a blinded judge (A.B.). The histopathological score was calculated by adding the scores for each criterion, leading to a maximum score of 6 points per mouse.

For sectioning and immunofluorescent staining of whole LNs, skin-draining LNs were excised from 11- to 12-week-old female Ccl19-Cre $ER\alpha^{fl/fl}$ and $ER\alpha^{fl/fl}$ mice, embedded in optimum cutting temperature compound (Thermo Fisher Scientific, Waltham, MA, USA) and flash-frozen. Frozen samples were cut into 7μm sections using a Cryostar NX70 (Epredia, Portsmouth, NH, USA). Sections were air-dried for 30 min, fixed in ice-cold acetone (Sigma Aldrich) for 7 min at −20°C and air-dried for a further 15 min. LN sections were circled with a barrier pen, rehydrated for 10 min in PBS and blocked with 5% goat serum (Nordic Biolabs, Täby, Sweden) in PBS for 20 min. Primary antibodies CD31 and podoplanin (BioLegend, San Diego, CA, USA) diluted in blocking buffer [0.2% Triton-X 100 (Sigma Aldrich) and 10% goat serum] were added, and the sections incubated at 4°C overnight. The following day, sections were washed with PBS. The secondary antibodies goat anti-rat Alexa 568 and goat anti-hamster Alexa 488 (Invitrogen, Waltham, MA, USA) diluted in PBS were added and the sections were incubated in the dark for 40 min at room temperature. Sections were washed with PBS, counterstained with Hoechst 33342 (Thermo Fisher Scientific) and mounted with Prolong Diamond Antifade mount (Thermo Fisher Scientific). The sections were imaged with an SP8 confocal microscope (Leica, Wetzlar, Germany), and the images were stitched and smoothed with LAS X version 3.5.5 software (Leica). Brightness and contrast were adjusted using Adobe Photoshop version 24.6.0 (Adobe, San Jose, CA, USA).

Preparation of single-cell suspensions from LNs

Collected skin-draining LNs were torn apart with forceps. Half of the LN fragments were squeezed through a 70-μm cell strainer, washed through with plain Roswell Park Memorial Institute (RPMI) without phenol red (Gibco) and counted with an automated cell counter (XP-300; Sysmex, Norderstedt, Germany). These cells were then used for flow cytometry analysis of T- and B-cell populations, and enzyme-linked immunospot assay of Ig-producing cells.

The remaining half of the dissected LNs were placed in the digestion buffer (RPMI supplemented with 2% fetal bovine serum (Sigma Aldrich), 0.8 mg mL^{-1} dispase II (Life Technologies, Carlsbad, CA, USA), 0.2 mg mL^{-1} collagenase P (Roche, St. Louis, MO, USA) and 0.1 mg mL^{-1} DNase I (Worthington Biochemical Corporation, Lakewood, NJ, USA) and digested for 20 min at 37°C while shaking. The samples were pipetted up and down after 20 min to aid digestion. The undigested fragments were allowed to settle and the supernatant was collected in a separate tube containing cold RPMI with 2% fetal bovine serum to stop digestion. The remaining fragments were again digested in the digestion buffer for 10 min at 37°C, vigorously pipetted and the supernatant was removed as before. Any remaining fragments were again digested in the digestion buffer for 10 min, with intermittent pipetting every 2 min. Once all fragments were digested, the washed supernatants were spun down at 300*g*, 4°C for 5 min, resuspended in PBS and counted using an automatic cell counter (Sysmex). These cells were then processed further for flow cytometry analysis of LN stromal cells, DCs and macrophages. Alternatively, digested cells were cultured for downstream quantitative PCR.

For the calculation of total cells per LN, cell counts from both fractions were added together and divided by the number of collected LNs for each mouse.

Flow cytometry

For analysis of LN macrophages and DCs in LNs, cells were stained with eFluor780-conjugated viability dye (Invitrogen), Fc-γ receptor block (Becton Dickinson, Franklin Lakes, NJ, USA) and the following fluorescently labeled antibodies: PDCA-1-PE (Bio129c; eBioscience, Affymetrix, Santa Clara, CA, USA), CD8-BV421 (53–6.7), CD11b-BV421 (M1/70), MHCII-BV510 (M5/114.15.2), CD11c-FITC (N418), CD169-PE (3D6.112), CD4-PECy7 (RM4-5), F4/80-PECy7 (BM8), CD86-PerCP (GL-1) and CD40-APC (3/23) (BioLegend).

For the analysis of FRCs in LNs, the cells were stained with eFluor780-conjugated viability dye (Invitrogen), Fc-γ receptor block (Becton Dickinson) and the following fluorescently labeled antibodies: CD31-BV421 (390), MHCII-BV510 (M5/114.15.2), CD45-FITC (30-F11), Ter-119-FITC (TER119), PD-L1-PE (10F.9G2), Podoplanin-PECy7 (8.1.1), CD86-PerCP (GL-1) and CD40-APC (3/23) (BioLegend).

For staining of intracellular cytokines in T cells in LNs, 2×10^6 cells were seeded in each well of a 24-well plate in complete media [RPMI-1640 without phenol red (Gibco) 10% fetal bovine serum, 1% penicillin/streptomycin (Sigma Aldrich)] together with 1% phorbol 12-myristate 13-acetate (Sigma Aldrich), 2% ionomycin (Sigma Aldrich) and 0.2% GolgiPlug (Becton Dickinson). The cells were then incubated for 4 h (37°C, 5% CO_2). After harvest, the cells were stained

with eFluor780-conjugated viability dye (Invitrogen), Fc-γ receptor block (Becton Dickinson) and the following fluorescently labeled extracellular antibodies: CD3ε-PECy7 (145-2C11) (BioLegend), CD4-PerCP (RM4-5), CD8-BV510 (53–6.7) and γδTCR-BV21 (GL3; all BioLegend). Cells were then fixed using the Intracellular Fixation Buffer kit (Thermo Fisher Scientific). For intracellular staining, cells were permeabilized with PERM-buffer (Thermo Fisher Scientific), incubated for 15 min at 4°C with Fc-γ receptor block and stained with the following fluorescently labeled intracellular antibodies: IFNγ-PE (281–2; Becton Dickinson), IL17A-APC (ebio8F10–3; Invitrogen) and IL4-AlexaFluor488 (11B11; BioLegend). For analysis of B cells in LNs, the cells were stained with eFluor780-conjugated viability dye (Invitrogen, Waltham, MA, USA), Fc-γ receptor block (Becton Dickinson) and the following fluorescently labeled antibodies: CD138-BV421 (281–2; Becton Dickinson), TACI-APC (ebio8F10–3; Invitrogen), CD19-BV510 (6D5), B220-PECy7 (RA3-6B2) and CD3ε-PECy7 (145-2C11) (BioLegend).

All cells were acquired using a FACSVerse (Becton Dickinson). Data were analyzed using FlowJo software version 10 (FlowJo, Ashland, OR, USA).

FRC cell cultures

Digested cells from skin-draining LNs were suspended in 1.5 mL αMEM culture media (Gibco) containing 20% fetal bovine serum (Sigma Aldrich) and 1% penicillin/streptomycin (Sigma Aldrich) and plated on 6-well plates at a concentration of 1×10^7 cells/well. Cells were incubated at 37°C, 5% CO_2. After 24 h, nonadherent cells were removed, the wells were washed with sterile PBS containing 50 μg mL^{-1} gentamicin (Gibco) and the culture media was replaced. Cells were then washed every 2 days for a total of 6–8 days. Upon reaching confluency, cells were either stimulated with 1×10^{-8} mol L^{-1} E2 (Sigma Aldrich), dissolved in absolute ethanol (ThermoFisher Scientific) and suspended in 1.5 mL of culture media, or left unstimulated (culture media replaced with 1.5 mL new culture media containing an equivalent volume of ethanol as added to the E2-stimulated cells). After 24 h, cells were lysed with 600 μL QIAzol reagent (Qiagen, Hilden, Germany) and stored at −80°C until further analysis.

Quantitative PCR

RNA from FRC cell lysate suspended in QIAzol was extracted using the RNeasy Mini Kit (Qiagen) according to the manufacturer's protocol. cDNA was constructed by reverse transcribing extracted RNA using the High-Capacity cDNA Reverse Transcription Kit (Applied Biosystems, Waltham, MA, USA). The quantitative PCR was performed with a predesigned probe for *Esr1* (Mm00433147_m1; Applied Biosystems) using StepOnePlus Real-Time PCR (Applied Biosystems). The abundance of *Esr1* messenger RNA was adjusted for the expression of 18S ribosomal RNA (4310893E; Applied Biosystems) and calculated with the ΔΔCT method.

Enzyme-linked immunospot assay

Enzyme-linked immunospot assay was used to determine the number of IgM- and IgG-secreting cells in LNs. In brief, 96-well mixed-cellulose plates (Merck Millipore, Burlington, MA, USA) were coated with 5 μg mL^{-1} goat anti-mouse IgM and IgG affinity-purified F(ab′)2 fragments (Organon Teknika Cappel, Jersey City, NJ, USA) in 50 μL PBS and incubated overnight in a humidity chamber at 4°C. The plates were then washed and blocked with 5% fetal bovine serum for 1 h. Single-cell suspensions from LNs were added at concentrations of 2×10^6, 1×10^6 and 2×10^5 cells mL^{-1}, 50 μL per well, and incubated at 37°C, 5% CO_2 for 3.5 h. Thereafter, 50 μL of diluted (1:750) alkaline phosphatase–conjugated goat anti-mouse IgG and IgM (Southern Biotech, Birmingham, AL, USA) were added to each well, and plates were incubated in a humidity chamber at 4°C overnight. The following day, plates were washed with distilled water and 80 μL of 5-bromo-4-chloro-3-indolyl phosphate solution (Sigma Aldrich) was added. Plates were incubated in the dark for up to an hour until dark purple spots formed, whereby the reaction was stopped with tap water and plates were allowed to dry before counting the spots.

Determination of cytokines

Cytokine concentration in serum was analyzed using the LEGENDplex Mouse B cell Panel – S/P (1-plex) w/VbP and the LEGENDplex Mouse Inflammation Panel (13-plex) w/VbP (BioLegend) according to the manufacturer's protocols. Data were acquired using a FACSVerse and analyzed with FlowJo software version 10.

Statistical analysis

All statistical analysis was conducted using GraphPad Prism 9 (GraphPad Software Inc., La Jolla, CA, USA). The unpaired two-tailed Student's *t*-test was used to compare two groups. Two-way ANOVA followed by Tukey's *post hoc* multiple comparison test was used to compare genotypes (ERα^fl/fl and Ccl19-Cre ERα^fl/fl) and treatment groups (Veh and E2). A P-value of less than 0.05 was considered to have statistical significance. Results of the two-way ANOVA are displayed above each graph with the corresponding P-value; T = treatment, G = genotype and Int = interaction term. Significant differences between individual groups after the *post hoc* analysis are denoted as follows: *$P < 0.05$; **$P < 0.01$; ***$P < 0.001$; ****$P < 0.0001$. Histopathological scoring is shown as the median score and analyzed with the Kruskal–Wallis test. All other data are displayed as mean ± standard error of the mean.

AUTHOR CONTRIBUTIONS

Aidan Barrett: Conceptualization; formal analysis; investigation; methodology; visualization; writing – original draft; writing – review and editing. **Karin Horkeby:** Investigation; writing – review and editing. **Carmen Corciulo:** Investigation; writing – review and editing. **Hans Carlsten:** Resources; writing – review and editing. **Marie K Lagerquist:** Resources; writing – review and editing. **Julia M Scheffler:** Conceptualization; formal analysis; investigation; methodology; supervision; visualization; writing – review and editing. **Ulrika Islander:** Conceptualization; formal analysis; funding acquisition; methodology; supervision; visualization; writing – original draft; writing – review and editing.

CONFLICT OF INTEREST

The authors declare that the research was conducted in the absence of any commercial or financial relationships that could be construed as a potential conflict of interest.

ETHICS APPROVAL AND CONSENT TO PARTICIPATE

All animal experiments in this study were performed in accordance with the ethical permit protocols approved by the Regional Ethical Review Board in Gothenburg, Sweden (Dnr: 4518/22).

DATA AVAILABILITY STATEMENT

The data that support the findings of this study are available from the corresponding author upon reasonable request.

REFERENCES

1. Doran MF, Pond GR, Crowson CS, O'Fallon WM, Gabriel SE. Trends in incidence and mortality in rheumatoid arthritis in Rochester, Minnesota, over a forty-year period. *Arthritis Rheum* 2002; **46**: 625–631.

2. Feldmann M, Brennan FM, Maini RN. Rheumatoid arthritis. *Cell* 1996; **85**: 307–310.

3. Goemaere S, Ackerman C, Goethals K, *et al.* Onset of symptoms of rheumatoid arthritis in relation to age, sex and menopausal transition. *J Rheumatol* 1990; **17**: 1620–1622.

4. Walitt B, Pettinger M, Weinstein A, *et al.* Effects of postmenopausal hormone therapy on rheumatoid arthritis: the women's health initiative randomized controlled trials. *Arthritis Rheum* 2008; **59**: 302–310.

5. D'Elia HF, Larsen A, Mattsson LA, *et al.* Influence of hormone replacement therapy on disease progression and bone mineral density in rheumatoid arthritis. *J Rheumatol* 2003; **30**: 1456–1463.

6. Hall GM, Daniels M, Huskisson EC, Spector TD. A randomised controlled trial of the effect of hormone replacement therapy on disease activity in postmenopausal rheumatoid arthritis. *Ann Rheum Dis* 1994; **53**: 112–116.

7. Orellana C, Saevarsdottir S, Klareskog L, Karlson EW, Alfredsson L, Bengtsson C. Postmenopausal hormone therapy and the risk of rheumatoid arthritis: results from the Swedish EIRA population-based case-control study. *Eur J Epidemiol* 2015; **30**: 449–457.

8. Ostensen M. Sex hormones and pregnancy in rheumatoid arthritis and systemic lupus erythematosus. *Ann NY Acad Sci* 1999; **876**: 131–143; discussion 144.

9. Jansson L, Holmdahl R. Oestrogen induced suppression of collagen arthritis. IV: progesterone alone does not affect the course of arthritis but enhances the oestrogen-mediated therapeutic effect. *J Reprod Immunol* 1989; **15**: 141–150.

10. Nandakumar KS, Svensson L, Holmdahl R. Collagen type II-specific monoclonal antibody-induced arthritis in mice: description of the disease and the influence of age, sex, and genes. *Am J Pathol* 2003; **163**: 1827–1837.

11. Jochems C, Islander U, Erlandsson M, *et al.* Effects of oestradiol and raloxifene on the induction and effector phases of experimental postmenopausal arthritis and secondary osteoporosis. *Clin Exp Immunol* 2011; **165**: 121–129.

12. Engdahl C, Jochems C, Windahl SH, *et al.* Amelioration of collagen-induced arthritis and immune-associated bone loss through signaling via estrogen receptor alpha, and not estrogen receptor beta or G protein-coupled receptor 30. *Arthritis Rheum* 2010; **62**: 524–533.

13. Engdahl C, Börjesson AE, Forsman HF, *et al.* The role of total and cartilage-specific estrogen receptor alpha expression for the ameliorating effect of estrogen treatment on arthritis. *Arthritis Res Ther* 2014; **16**: R150.

14. Straub RH. The complex role of estrogens in inflammation. *Endocr Rev* 2007; **28**: 521–574.

15. Cutolo M, Straub RH. Sex steroids and autoimmune rheumatic diseases: state of the art. *Nat Rev Rheumatol* 2020; **16**: 628–644.

16. Medina KL, Strasser A, Kincade PW. Estrogen influences the differentiation, proliferation, and survival of early B-lineage precursors. *Blood* 2000; **95**: 2059–2067.

17. Kincade PW, Smithson G. Sex hormones as negative regulators of lymphopoiesis. *Immunol Rev* 1994; **137**: 119–134.

18. Rijhsinghani AG, Thompson K, Bhatia SK, Waldschmidt TJ. Estrogen blocks early T cell development in the thymus. *Am J Reprod Immunol* 1996; **36**: 269–277.

19. Gustafsson KL, Nilsson KH, Farman HH, *et al.* ERα expression in T lymphocytes is dispensable for estrogenic effects in bone. *J Endocrinol* 2018; **238**: 129–136.

20. Fujiwara Y, Piemontese M, Liu Y, Thostenson JD, Xiong J, O'Brien CA. RANKL (receptor activator of NFκB ligand) produced by osteocytes is required for the increase in B cells and bone loss caused by estrogen deficiency in mice. *J Biol Chem* 2016; **291**: 24838–24850.

21. Bernardi AI, Andersson A, Grahnemo L, *et al.* Effects of lasofoxifene and bazedoxifene on B cell development and function. *Immun Inflamm Dis* 2014; **2**: 214–225.

22. Andersson A, Stubelius A, Karlsson MN, *et al.* Estrogen regulates T helper 17 phenotype and localization in experimental autoimmune arthritis. *Arthritis Res Ther* 2015; **17**: 32.

23. Lütge M, Pikor NB, Ludewig B. Differentiation and activation of fibroblastic reticular cells. *Immunol Rev* 2021; **302**: 32–46.

24. Fletcher AL, Acton SE, Knoblich K. Lymph node fibroblastic reticular cells in health and disease. *Nat Rev Immunol* 2015; **15**: 350–361.

25. Denton AE, Roberts EW, Linterman MA, Fearon DT. Fibroblastic reticular cells of the lymph node are required for retention of resting but not activated CD8$^+$ T cells. *Proc Natl Acad Sci USA* 2014; **111**: 12139–12144.

26. Nakayama Y, Brinkman CC, Bromberg JS. Murine fibroblastic reticular cells from lymph node interact with CD4$^+$ T cells through CD40-CD40L. *Transplantation* 2015; **99**: 1561–1567.

27. Onder L, Cheng HW, Ludewig B. Visualization and functional characterization of lymphoid organ fibroblasts. *Immunol Rev* 2022; **306**: 108–122.

28. Koliaraki V, Prados A, Armaka M, Kollias G. The mesenchymal context in inflammation, immunity and cancer. *Nat Immunol* 2020; **21**: 974–982.

29. D'Rozario J, Knoblich K, Lütge M, *et al.* Fibroblastic reticular cells provide a supportive niche for lymph node-resident macrophages. *Eur J Immunol* 2023; **53**: e2250355.

30. Wiechers C, Pezoldt J, Beckstette M, Berner J, Schraml BU, Huehn J. Lymph node stromal cells support the maturation of pre-DCs into cDC-like cells via colony-stimulating factor 1. *Immunology* 2022; **166**: 475–491.

31. Bellomo A, Gentek R, Bajénoff M, Baratin M. Lymph node macrophages: scavengers, immune sentinels and trophic effectors. *Cell Immunol* 2018; **330**: 168–174.

32. Phan TG, Green JA, Gray EE, Xu Y, Cyster JG. Immune complex relay by subcapsular sinus macrophages and noncognate B cells drives antibody affinity maturation. *Nat Immunol* 2009; **10**: 786–793.

33. Alexandre YO, Devi S, Park SL, Mackay LK, Heath WR, Mueller SN. Systemic inflammation suppresses lymphoid tissue remodeling and B cell immunity during concomitant local infection. *Cell Rep* 2020; **33**: 108567.

34. Novkovic M, Onder L, Cupovic J, *et al.* Topological small-world organization of the fibroblastic reticular cell network determines lymph node functionality. *PLoS Biol* 2016; **14**: e1002515.

35. Pikor NB, Mörbe U, Lütge M, *et al.* Remodeling of light and dark zone follicular dendritic cells governs germinal center responses. *Nat Immunol* 2020; **21**: 649–659.

36. Lee MH, Chakhtoura M, Sriram U, Caricchio R, Gallucci S. Conventional DCs from male and female lupus-prone B6.NZM Sle1/Sle2/Sle3 mice express an IFN signature and have a higher immunometabolism that are enhanced by estrogen. *J Immunol Res* 2018; **2018**: 1–21.

37. Andersson A, Grahnemo L, Engdahl C, *et al.* IL-17-producing γδT cells are regulated by estrogen during development of experimental arthritis. *Clin Immunol* 2015; **161**: 324–332.

38. Medina KL, Kincade PW. Pregnancy-related steroids are potential negative regulators of B lymphopoiesis. *Proc Natl Acad Sci USA* 1994; **91**: 5382–5386.

39. Verthelyi DI, Ahmed SA. Estrogen increases the number of plasma cells and enhances their autoantibody production in nonautoimmune C57BL/6 mice. *Cell Immunol* 1998; **189**: 125–134.

40. Huang HY, Rivas-Caicedo A, Renevey F, *et al.* Identification of a new subset of lymph node stromal cells involved in regulating plasma cell homeostasis. *Proc Natl Acad Sci USA* 2018; **115**: E6826–E6835.

41. Batten M, Groom J, Cachero TG, *et al.* BAFF mediates survival of peripheral immature B lymphocytes. *J Exp Med* 2000; **192**: 1453–1466.

42. Kovats S. Estrogen receptors regulate innate immune cells and signaling pathways. *Cell Immunol* 2015; **294**: 63–69.

43. Miller RAJ, Williams AP, Kovats S. Sex chromosome complement and sex steroid signaling underlie sex differences in immunity to respiratory virus infection. *Front Pharmacol* 2023; **14**: 1150282.

44. Ludewig B, Chai Q, Onder L, *et al.* CCL19-Cre transgenics: targeting lymph node fibroblastic reticular cells *in vivo* (44.14). *J Immunol* 2012; **188**: 44.14.

45. Antonson P, Omoto Y, Humire P, Gustafsson J. Generation of ERα-floxed and knockout mice using the Cre/LoxP system. *Biochem Biophys Res Commun* 2012; **424**: 710–716.

SUPPORTING INFORMATION

Additional supporting information may be found online in the Supporting Information section at the end of the article.